Analog Integrated Circuits and Signal Processing (2019) 100:269–277
https://doi.org/10.1007/s10470-019-01457-3

Active biquad tunable filter design

Debadipta Basak[1] · Koelgeet Kaur[1] · Subir Kumar Sarkar[1]

Received: 1 November 2018 / Revised: 19 February 2019 / Accepted: 16 April 2019 / Published online: 6 May 2019

Abstract
This paper presents the technique of single differential stage op-amp which is used for the active biquad filter design with the inclusion of buffers at the output of op-amp. This procedure provides the advantage of low power and low area requirement with reduction of propagation delay. The buffer circuit proffers the tunability of the filter by modulating the transconductance of the output buffer. This approach has been established to design a second order active biquad filter. The two biquad high pass and low pass sections are used to design a fourth order band pass and band stop filter with 0.18 μm CMOS process technology which consumes significantly less power than conventional approaches.

Keywords Biquad · Low area · Low power · Tunability

1 Introduction

Requirement for more functionality and improvement of performance led to increase in power consumption on the contrary to advancement of the system. Therefore the need for low power circuits have become very much salient in the design techniques. Application of active RC filters are very common in the system designs and for this reason RC filters must consume less power and retain less chip area.

Unlike Gm-C filters, active RC filters have higher linearity due to the fact that the op-amps used here as integrators are connected in closed loop [1]. As op-amps are major active component, so it has a huge participation in the power consumption of the filter circuit. Area [2] occupied by the filter also increases due to the use of capacitor banks for tuning purpose.

Some methods aimed to achieve the aforementioned criteria are replica circuit for tuning [1], anti-pole splitting technique [3], technique explained in [4] to achieve low power op-amp by making concessions at linearity etc.

Here the technique used in [5] to reduce the power consumption and area requirement has been adopted. Instead of conventional op-amp with multiple stages, single stage op-amp is used in this work. Thus the need for capacitor banks and compensation capacitors are discarded which eventually helps in reduction of area requirement. In this design technique a single differential stage op-amp is applied to build an active biquad high pass filter (HPF) and by cascading the HPF along with low pass filter obtained from [5], a BPF is designed. A specific buffer circuit is used to perform the tuning operation of the filter while retaining the low power characteristics.

2 Biquad section

In the present investigation a fully differential single stage opamp [5, 6] has been considered for the design of the active biquad filter [7]. The single stage opamp requires less area compared to multistage opamp and it also eliminates the extra area occupied by capacitor banks and compensation capacitors.

The active biquad filter involves transfer function to be the ratio of two quadratic functions of the complex variables. The general expression for the second order or

✉ Debadipta Basak
db.rini1991@gmail.com

Koelgeet Kaur
koelgeetkaur45@gmail.com

Subir Kumar Sarkar
su_sircir@yahoo.co.in

[1] Department of Electronics and Telecommunication Engineering, Jadavpur University, 188, Raja S.C. Mallick Rd, Kolkata 700032, India

biquadratic transfer function is usually expressed in the standard form as:

$$H(s) = \frac{a_2 s^2 + a_1 s + a_0}{s^2 + s\left(\frac{w_0}{Q}\right) + w_0^2} \tag{1}$$

The biquad HPF is shown in Fig. 1(b) with the transfer function given by (1).

$$\frac{V_{out}}{V_{in}} = \frac{\frac{R_3}{R_1 R_{in}} s^2}{s^2 + \frac{Q}{w_0} s + w_0^2} \tag{2}$$

where $w_0 = \sqrt{\frac{R_3}{R_1 R_2 R_{in} C_1 C_2}}$ and $Q = \frac{R_3}{R_1 R_2 C_2} + \frac{1}{C_1 R_{in}}$.

So the transfer function becomes

$$\frac{V_{out}}{V_{in}} = \frac{\frac{R_3}{R_1 R_{in}} s^2}{s^2 + \left(\frac{R_3}{R_1 R_2 C_2} + \frac{1}{C_1 R_{in}}\right) s + \frac{R_3}{R_1 R_2 R_{in} C_1 C_2}} \tag{3}$$

In addition to this, it is considered that the output of each op-amp is attached to a buffer circuit with gain 1/n1 and 1/n2 respectively. Figure 2 depicts the active high pass filter with buffer between the output of each op-amp and the feedback path. As a result the output voltage of each op-amp is divided by $n_i > 1$ (general case) and the transfer function gets modified as the following (4).

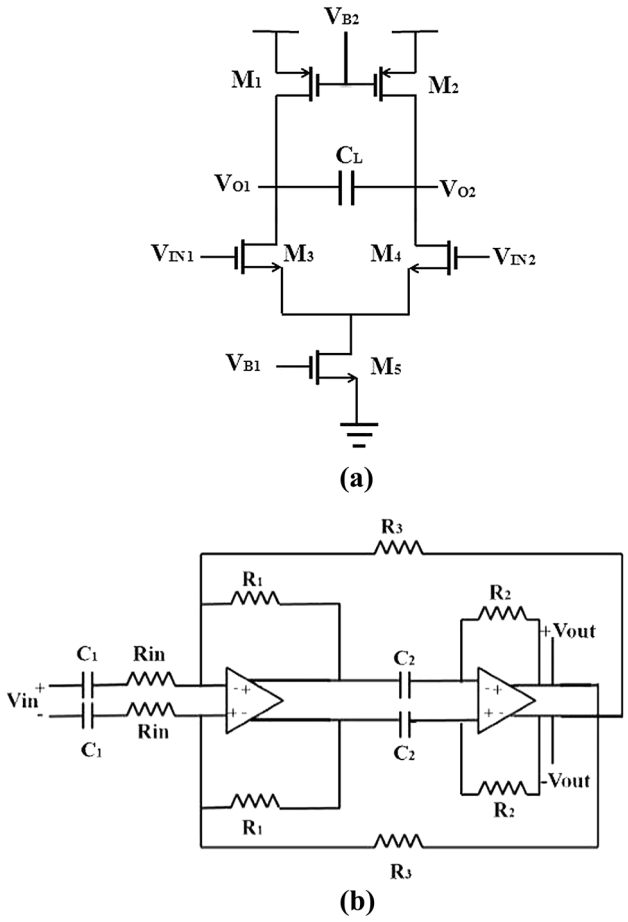

Fig. 1 **a** Fully differential single stage op-amp circuit, **b** biquad high pass filter

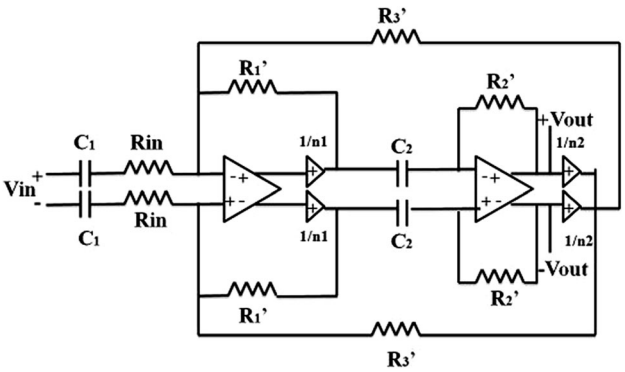

Fig. 2 Biquad high pass filter with buffer

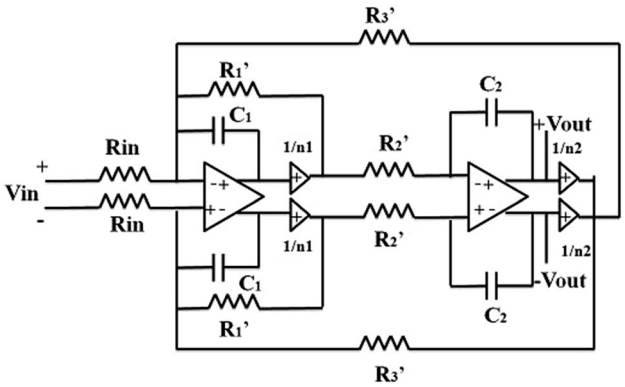

Fig. 3 Biquad low pass filter with buffer

$$\frac{V_{out}}{V_{in}} = \frac{\frac{n_2 R_3'}{n_1 R_1' R_{in}} s^2}{s^2 + \left(\frac{R_3'}{n_1 R_1' R_2' C_2} + \frac{1}{C_1 R_{in}}\right) s + \frac{R_3'}{n_1 R_1' R_2' R_{in} C_1 C_2}} \tag{4}$$

where $w_0 = \sqrt{\frac{R_3'}{n_1 R_1' R_2' R_{in} C_1 C_2}}$, $Q = \frac{R_3'}{n_1 R_1' R_2' C_2} + \frac{1}{C_1 R_{in}}$ and $R_i' = \frac{R_i}{n_i}$(general case).

The benefit of the revised circuit is as follows

1. The output is separated from the feedback resistor that eliminates the requirement the of compensated capacitor.
2. The power consumption reduces as single stage op-amp is applied.
3. The pole location can be adjusted by n and the use of capacitor bank can be avoided.

The low pass biquad filter design with buffer implemented at the output is described in [5] and the transfer function is given by (5).

$$\frac{V_{out}}{V_{in}} = \frac{\frac{1}{n_1 R_2' R_{in} C_1 C_2}}{s^2 + \frac{1}{n_1 R_1' C_1} s + \frac{1}{n_1 n_2 R_2' R_3' C_1 C_2}} \tag{5}$$

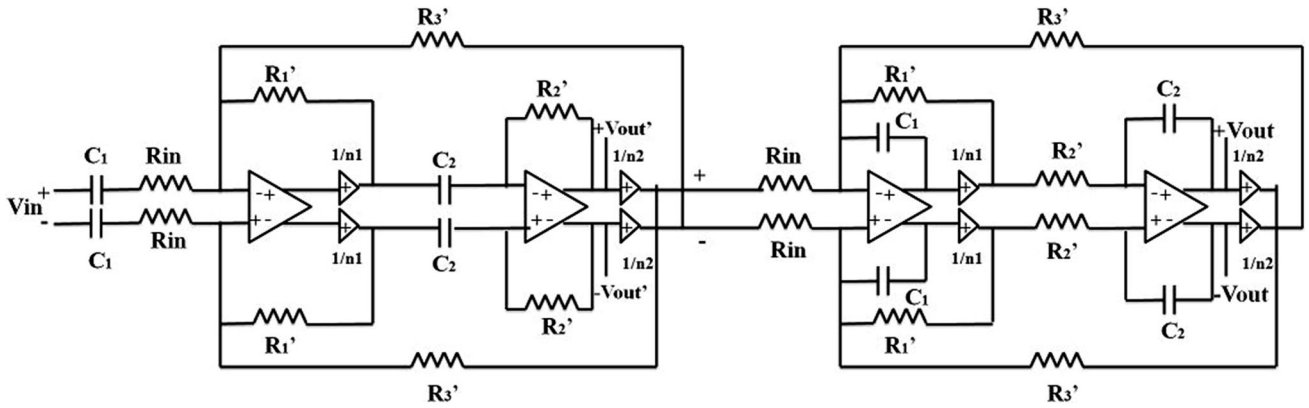

Fig. 4 Biquad BPF with buffer which is cascade of HPF followed by a LPF

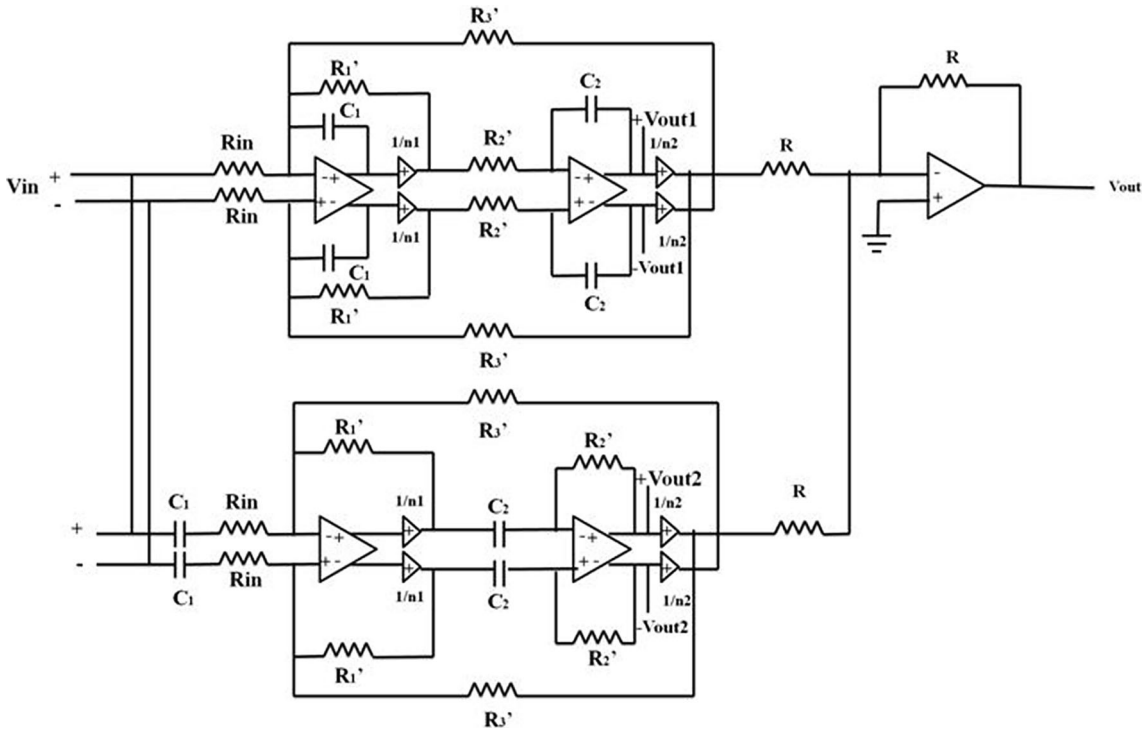

Fig. 5 Biquad band stop filter with buffer which is HPF and LPF connected in parallel followed by a summer circuit

Figure 4 depicts the biquad low pass filter with buffer inclusion.

These two circuits of Figs. 2 and 3 are cascaded to design a band pass filter shown in Fig. 4 and as the two biquads are in cascade so the transfer function of the resultant circuit is derived to be of 4th order. The transfer function of the same is given by (6).

Here the resistors R_2'–R_4' and R_6'–R_8' are same as R_2–R_4 and R_5–R_8 but they are divided by n_i only.

The HPF and the LPF are connected in parallel and the output of both the filters are supplied to a summer circuit to construct a band stop filter shown in Fig. 5. The overall transfer function of the band stop filter with the buffer circuit connected at the op-amp output is derived in (7).

$$\frac{V_{out}}{V_{in}} = \frac{\frac{R_3'}{n_3 R_1 R_4' R_5 R_8' C_3 C_4}}{\left[s^2 + \left(\frac{R_3'}{n_1 R_2^1 R_4' C_2} + \frac{1}{R_1 C_1}\right)s + \frac{R_3'}{n_1 R_1 R_2^1 R_4' C_1 C_2}\right]\left[s^2 + \frac{1}{n_3 R_6' C_3}s + \frac{1}{n_3 n_4 R_7' R_8' C_3 C_4}\right]} \quad (6)$$

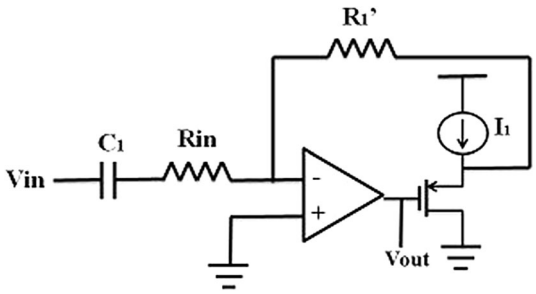

Fig. 6 Source follower buffer circuit connected between op-amp output and feedback resistor

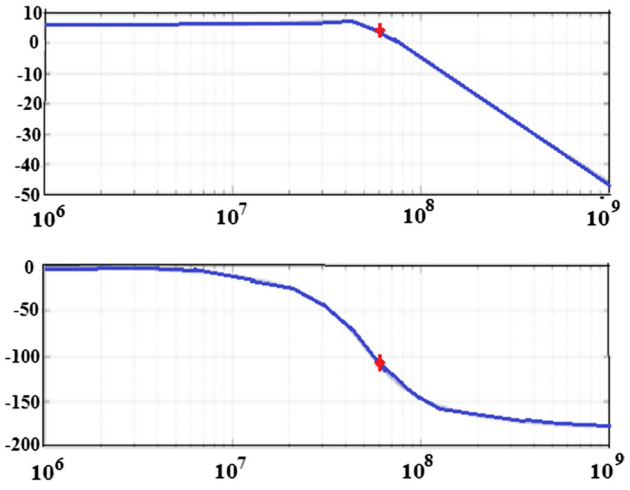

Fig. 7 Magnitude and phase response of LPF

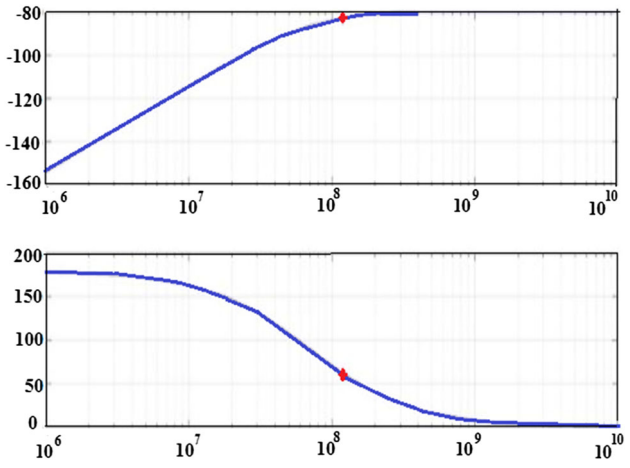

Fig. 8 Magnitude and phase response of HPF

$$\frac{V_{out}}{V_{in}} = \left[\frac{\frac{1}{n_3 R_5 R_8' C_3 C_4}}{\left[s^2 + \frac{1}{n_3 R_6' C_3} s + \frac{1}{n_3 n_4 R_7' R_8' C_3 C_4}\right]}\right] + \left[\frac{\frac{n_2 R_3'}{n_1 R_1 R_2'} s^2}{\left[s^2 + \left(\frac{R_3'}{n_1 R_2' R_4' C_2} + \frac{1}{R_1 C_1}\right) s + \frac{R_3'}{n_1 R_1 R_2' R_4' C_1 C_2}\right]}\right] \quad (7)$$

The buffer circuit that provides ($1/n_i$) gain stage is constructed by a source follower circuit implemented between the output of each op-amp and the feedback path. The buffer circuit for the lossy differentiator is given by the Fig. 6. The gain stage parameter ni is derived as

$$n_i = 1 + \frac{1}{g_{mBuffer} R_1'}$$

where $g_{mBuffer}$ is the transconductance of buffer MOSFET. So by controlling the MOSFET parameters and the current of the source follower, we can control transconductance of the buffer which in turn can control the value of n_i. The value of n_i thus works as the tuning parameter of the circuit and the pole locations of the filter can be tuned in accordance with the requirements. Thus the need for conventional tuning circuits for the filters can be eliminated.

3 Results and discussion

This section describes the magnitude plot of each of the filters with their cut off frequencies. The bandwidth of BPF and BSF matches close to the overlap of cutoff frequencies of the LPF and HPF.

The comparison with the conventional method and the tenability of the filter circuits are also investigated in this section.

3.1 Low pass filter

The magnitude and phase response of the fully differential LPF is as shown in the Fig. 7.

From the above response it is evident that the cut-off frequency (f_L) of the LPF is 60 MHz.

3.2 High pass filter

The magnitude and phase response of the fully differential HPF is as shown below.

From the above graph it is visible that the cut-off frequency (f_H) of the HPF is 20 MHz (Figs. 8, 9).

3.3 Band pass filter

Now, the second order low pass and high pass filter are cascaded to design the fourth order band pass filter, the

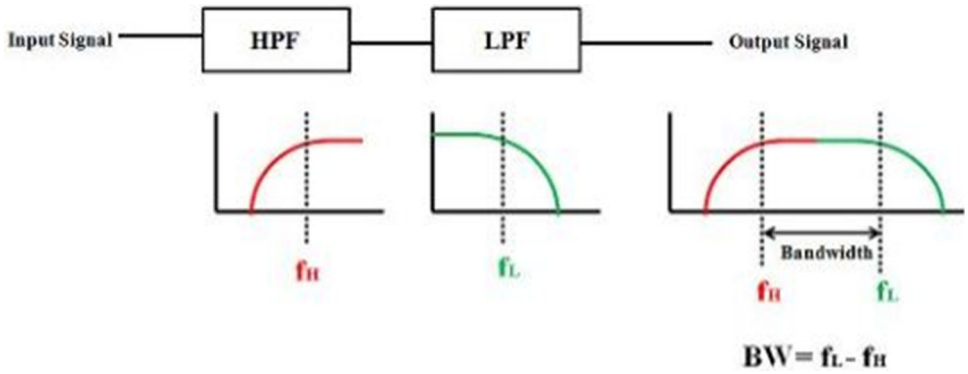

Fig. 9 Block diagram of BPF

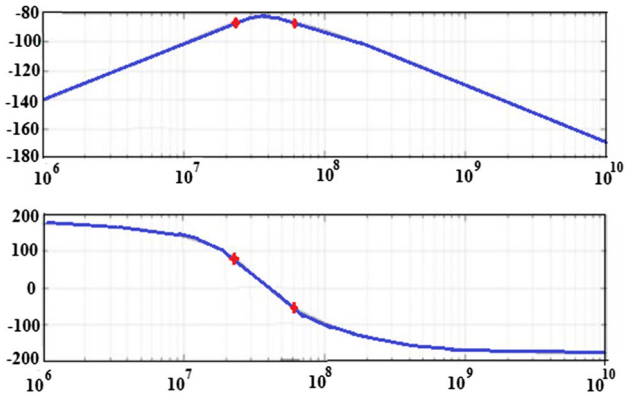

Fig. 10 Magnitude and phase plot of BPF

block diagram and the magnitude and phase response of the same is as shown in the Fig. 10.

The bandwidth of the band pass filter is calculated by the formula, $B \cdot W = f_L - f_H$, which is equal to 40 MHz. From the above graph in Fig. 10 it is observed that the bandwidth of the band pass filter is approx. 40 MHz.

3.4 Band stop filter

By connecting the second order low pass and high pass filter in parallel we can design the fourth order band stop filter, the block diagram and the magnitude and phase response of the same is illustrated in Figs. 11 and 12.

The bandwidth of the band stop filter is calculated by the formula, $B \cdot W = f_H - f_L$, which is equal to 44 MHz, and it is also evident from the graph in Fig. 12 (Table 1).

The above table makes a comparative study of the proposed method of designing filters and the conventional method in terms of average power, area occupancy and delay. This work suggests consumption of less area and low power along with the speed improvement.

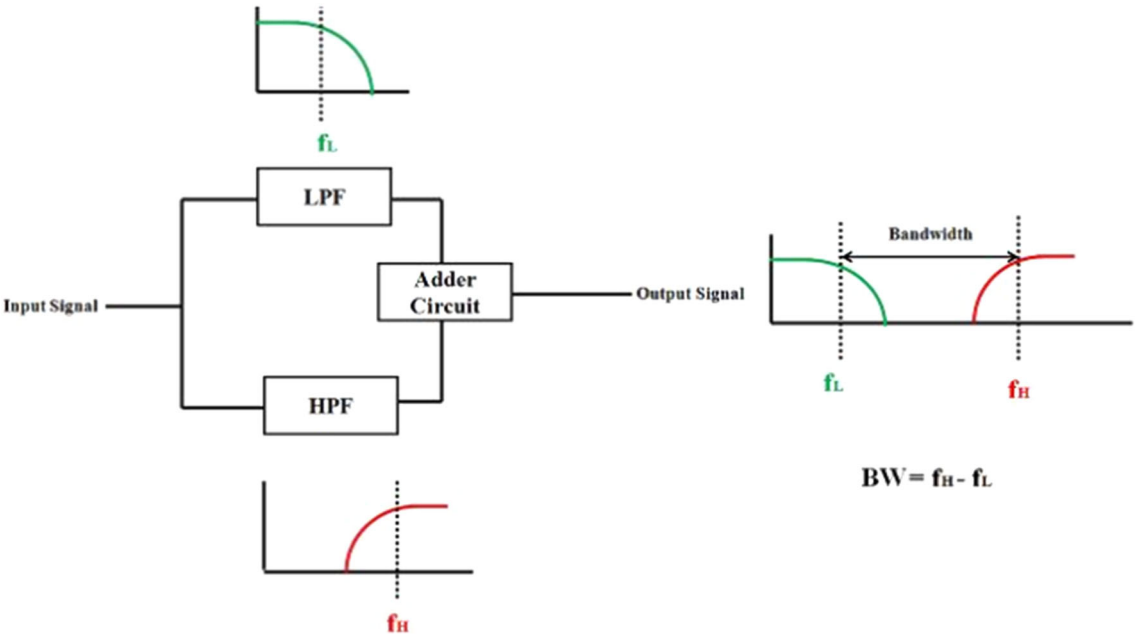

Fig. 11 Block diagram of BSP

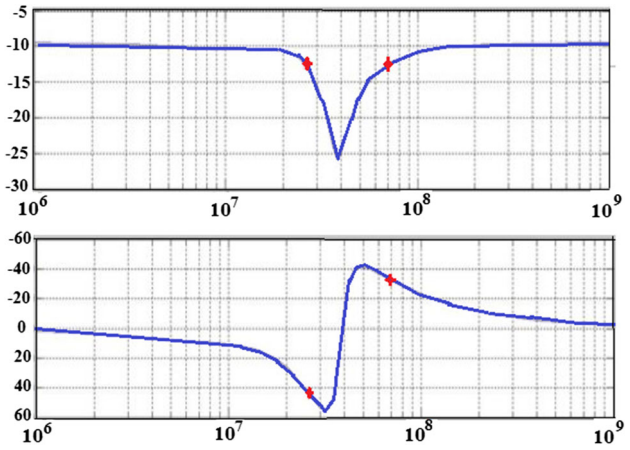

Fig. 12 Magnitude and phase plot of BSF

The data measured are from the simulation results of the circuits in Cadence. The input voltage provided was sinusoid of 0.5 V amplitude with varying frequencies in accordance with the filter pass band. V_{DD} is taken to be 1.8 V along with 0.18 μm CMOS process technology. The values of capacitances and resistances are considered as 1 pF and 10 KΩ respectively (Figs. 13, 14, 15).

By varying the current through the source follower buffer we can vary the value of n_i which is the key parameter for the changes in the transfer characteristics. The modulation technique in the voltage transfer characteristics of the biquad HPF with buffer added to opamp output has been shown in the following Fig. 16.

Thus by varying the value of n_i we can vary the cutoff frequencies of LPF and HPF. As a result the bandwidth of the BPF and the BSF can be varied accordingly. This modulation is illustrated in Table 2. Table 3 exhibits the comparison of this work with some other techniques published earlier. The positive gain margins (GM) and phase margins (PM) of the BPF and BSF for n = 2, 3 establishes the fact that the filters are stable even in low bandwidth that is shown in Table 4.

$$FOM = \frac{power \times area}{order \times Bandwidth \times SFDR \times IIP3}$$

Figure 17 exhibits the measured equivalent noise voltage of the filter that is found to be approximately 128 nV/$\sqrt{}$Hz. IIP3 of the filter is measured to determine the linearity of the filter. Figure 18 depicts the IIP3 of BPF at 28.5 dBm and Fig. 19 shows the same of BSF at 28 dBm.

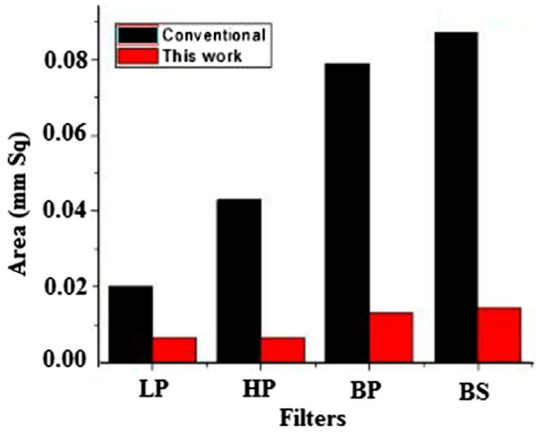

Fig. 13 The comparison of area occupied by the filters of this work and the conventional one

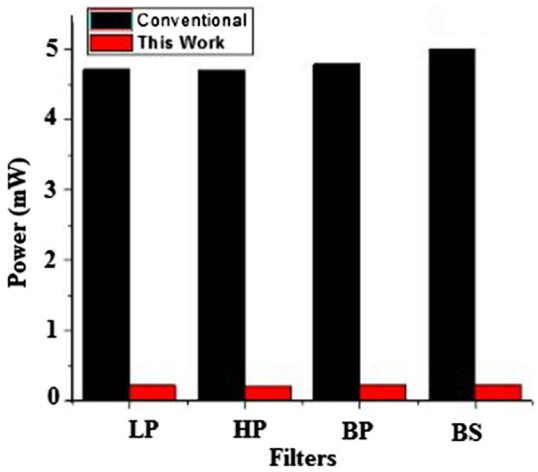

Fig. 14 The comparison of average power consumed by the filters of this work and the conventional one

4 Conclusion

A new technique to design filters with low power, low area and enhanced speed filters has been conferred in this paper. It has been investigated in this work that by incorporating a source follower circuit that works as a buffer at the output

Table 1 Comparison between this work and conventional method

Filter	This work			Filter with multi stage opamp [8]		
	Pavg (mW)	Area (mm^2)	Delay (nS)	Pavg (mW)	Area (mm^2)	Delay (nS)
LPF	0.219	0.0065	2.10	4.72	0.02	3.62
HPF	0.21	0.0065	1.09	4.71	0.043	2.01
BPF	0.23	0.013	3.2	4.79	0.0797	8.52
BSF	0.229	0.0145	4.3	5	0.087	9.6

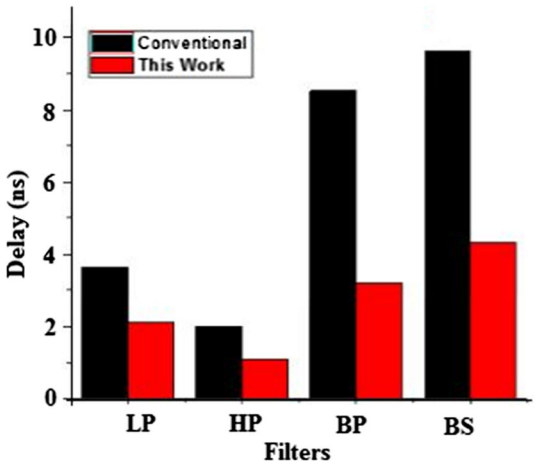

Fig. 15 The comparison of propagation delay of the filters of this work and the conventional one

of the opamp, the resistive load can be isolated from the output. The advantage of this technique can be observed in terms of tuning of the voltage transfer characteristics to desired value and low power operation of the circuit due to use of single differential stage of op-amp. The current through the buffer is adjusted which in turn controls the pole locations of the filter. It has been shown that by the proposed method low power, low area with increased speed tunable biquad high pass filter can be designed. Consequently we can therefore design band pass and band stop filters with higher orders that exhibit better performance

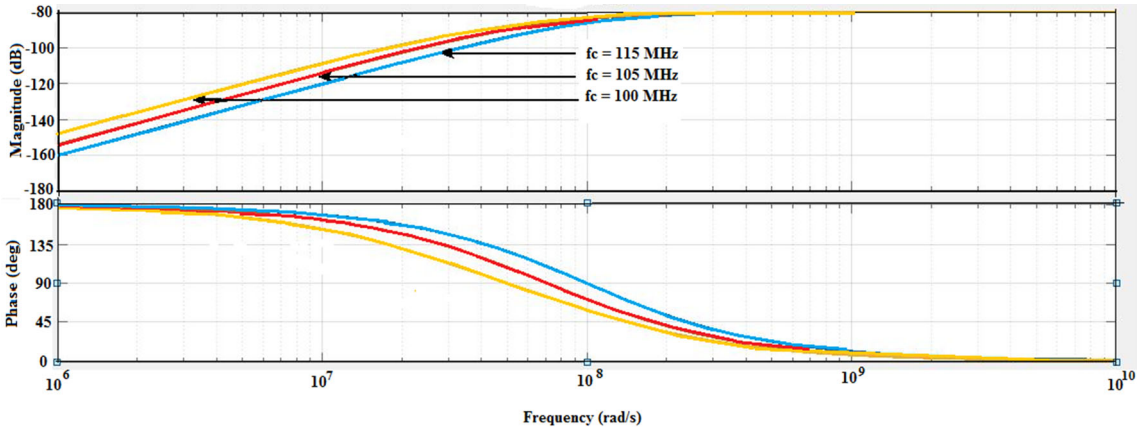

Fig. 16 Modulation of magnitude and phase plot of HPF

Table 2 Modulation of cutoff frequencies and bandwidths of the filters

f_{cl} (MHz)	f_{ch} (MHz)	f_{cl} (MHz)	f_{ch} (MHz)	Pass band (MHz)	Stop band (MHz)
$f_{cl1} = 84$	$f_{ch1} = 32$	$f_{cl3} = 65$	$f_{ch3} = 115$	f_{cl1}–$f_{ch1} = 52$	f_{ch3}–$f_{cl3} = 50$
$f_{cl2} = 79$	$f_{ch2} = 25$	$f_{cl4} = 43$	$f_{ch4} = 105$	f_{cl2}–$f_{ch2} = 54$	f_{ch4}–$f_{cl4} = 62$

Table 3 Comparison with some other techniques

Specification	[9]	[3]	[1]	[10]	[5]	This work
Technique	Gm-C	Active RC	Active RC	Active RC + DT	Active RC	Active RC
Technology (μm)	0.18	0.12	0.13	0.065	0.18	0.18
Order	3	5	5	4	4	4
SFDR (dB)	57.3	73	69	58	65.6	68.5
Input noise nV/$\sqrt{}$Hz	425	140	30	22.8	126	128
Power (mW) @VDD	4.1@1.2	6.1@1	11.25@1.5	10.8@1.8	0.5@1.8	0.23@1.8
Area (mm^2)	0.23	0.25	0.2	0.75	0.14	0.013
IIP3(dBm)	22.3	20	18.3	11	25	28.5
FOM (fJ μm^2)	6900	30.5	42.6	25,493	25.4	72.7

Table 4 Stability in low bandwidth of the filters

n values	BPF			BSF		
	BW (MHz)	GM (dB)	PM (°)	BW (MHz)	GM (dB)	PM (°)
2	28.02	1.25	43.196	19.64	8.56	81.73
3	26.8	1.96	49.605	18.01	8.15	65.45

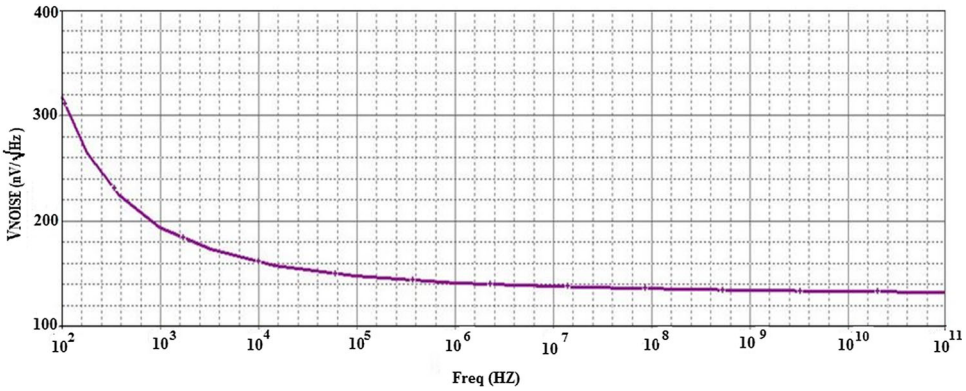

Fig. 17 Measured input equivalent noise voltage

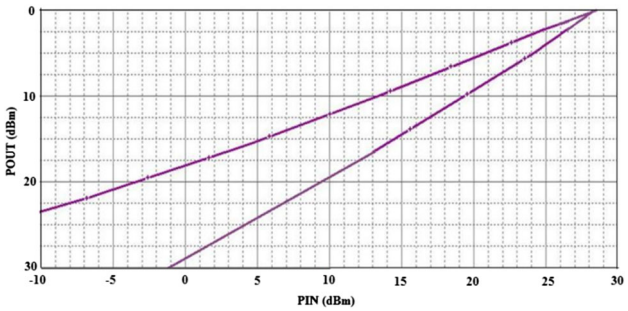

Fig. 18 Measured IIP3 of the BPF

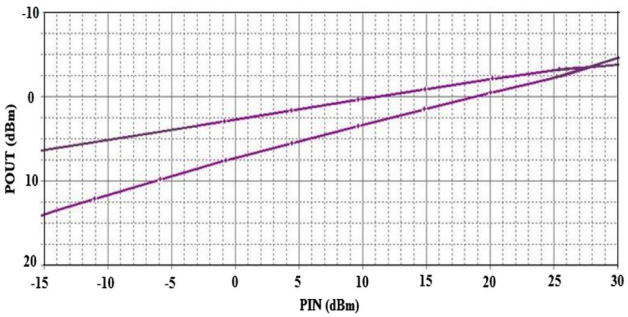

Fig. 19 Measured IIP3 of the BSF

compared to other filters designed using conventional 2 stage op-amp methods.

Acknowledgements The authors of this paper are thankful to the IC Centre of Jadavpur University, Kolkata for providing the access to the required software.

References

1. Kousai, S., Hamada, M., Ito, R., & Itakura, T. (2007). A 19.7 MHz, fifthorder active-RC Chebyshev LPF for draft IEEE802.11n with automatic quality-factor tuning scheme. *IEEE Journal of Solid-State Circuits, 42*(11), 2326–2337.
2. Hollman, T., Lindfors, S., Lansirinne, M., Jussila, J., & Halonen, K. A. I. (2001). A 2.7-V CMOS dual-mode baseband filter for PDC and WCDMA. *IEEE Journal of Solid-State Circuits, 36*(7), 1148–1153.
3. Vasilopoulos, A., Vitzilaios, G., Theodoratos, G., & Papananos, Y. (2006). A low-power wideband reconfigurable integrated active-RC filter with 73 dB SFDR. *IEEE Journal of Solid-State Circuits, 41*(9), 1997–2008.
4. Ye, L., Shi, C., Liao, H., Huang, R., & Wang, Y. (2013). Highly power-efficient active-RC filters with wide bandwidth-range using low-gain push-pull opamps. *IEEE Transactions on Circuits and Systems I: Regular Papers, 60*(1), 95–107.
5. Rasekh, A., & Sharif-Bakhtiar, M. (2018). Design of low-power low-area tunable active RC filters. *IEEE Transactions on Circuits and Systems—II: Express Briefs, 65*(1), 6–10.
6. Almutairi, F. T., & Karsilayan, A. I. (2019). Fully-differential second-order tunable bandstop filter based on source follower. *Electronics Letters, 55*(3), 122–124. https://doi.org/10.1049/el.2018.7496.
7. Wang, Y., Ye, L., Liao, H., Huang, R., & Wang, Y. (2015). Highly reconfigurable analog baseband for multistandard wireless receivers in 65-nm CMOS. *IEEE Transactions on Circuits and Systems II: Express Briefs, 62*(3), 296–300.
8. Hamzah, M. H., Jambek, A. B., & Hashim, U. (2014). Design and analysis of a two-stage CMOS op-amp using Silterra's 0.13 μm technology. In *2014 IEEE symposium on computer applications and industrial electronics (ISCAIE), Penang* (pp. 55–59). https://doi.org/10.1109/iscaie.2014.7010209.
9. Lo, T.-Y., Hung, C.-C., & Ismail, M. (2009). A wide tuning range Gm-C filter for multi-mode CMOS direct-conversion wireless receivers. *IEEE Journal of Solid-State Circuits, 44*(9), 2515–2524.
10. Shin, S.-H., et al. (2015). A 0.7-MHz-10-MHz CT + DT hybrid baseband chain with improved passband flatness for LTE

application. *IEEE Transactions on Circuits and Systems, 62*(1), 244–253.

Debadipta Basak is currently pursuing M.Tech. in VLSI and microelectronics from Jadavpur University, Kolkata, India. Her research areas include design of VLSI devices and analog integrated circuits.

Koelgeet Kaur is currently pursuing M.Tech. in VLSI and Micro Electronics at Jadavpur University, Kolkata, India. Her areas of research include VLSI device design, analog integrated circuits design.

Subir Kumar Sarkar (SM'09) received the Ph.D. (Tech.) degree in microelectronics from the University of Calcutta, Kolkata, India. He is currently a Professor with the Department of Electronics and Telecommunication Engineering, Jadavpur University, Kolkata.